Provided for non-commercial research and education use.
Not for reproduction, distribution or commercial use.

This article appeared in a journal published by Elsevier. The attached copy is furnished to the author for internal non-commercial research and education use, including for instruction at the authors institution and sharing with colleagues.

Other uses, including reproduction and distribution, or selling or licensing copies, or posting to personal, institutional or third party websites are prohibited.

In most cases authors are permitted to post their version of the article (e.g. in Word or Tex form) to their personal website or institutional repository. Authors requiring further information regarding Elsevier's archiving and manuscript policies are encouraged to visit:

http://www.elsevier.com/copyright

Author's personal copy

Applied Surface Science 258 (2011) 461–465

Contents lists available at SciVerse ScienceDirect

Applied Surface Science

journal homepage: www.elsevier.com/locate/apsusc

Enhancing photoresponse time of low cost Pd/ZnO nanorods prepared by thermal evaporation techniques for UV detection

H.I. Abdulgafour*, Z. Hassan, F.K. Yam, K. AL-Heuseen, Y. Yusof

School of Physics, Universiti Sains Malaysia, 11800 Penang, Malaysia

ARTICLE INFO

Article history:
Received 14 June 2011
Received in revised form 19 August 2011
Accepted 23 August 2011
Available online 30 August 2011

Keywords:
ZnO
Photodetector
Thermionic emission
Responsivity

ABSTRACT

High quality undoped ZnO nanorods have been synthesized at 850 °C by vapor–solid (VS) technique without a catalyst through a low cost process on silicon substrates. Then, ZnO nanorods have been characterized by using scanning electron microscopy (SEM), X-ray diffractometer (XRD), and photoluminescence (PL) spectroscopy. Metal–semiconductor–metal (MSM) photodetectors with palladium (Pd) as contact electrodes have been successfully constructed for ultraviolet (UV) detection. Under dark and UV illumination, the load resistance of the Pd/ZnO junction was found to be 80.4 kΩ, and 23.5 kΩ referring to the maximum allowed bias voltage; the barrier height was estimated to be about 0.8 eV, and 0.76 eV, at 5 V applied bias voltage, respectively. It was found that the maximum responsivity of the Pd/ZnO MSM photodetector was 0.106 A/W at 300 nm which corresponds to a quantum efficiency of 43.8% at 5 V applied bias voltage. The transient photoresponse of the fabricated device is reported under different applied biases at 1 V, 3 V, and 5 V.

© 2011 Elsevier B.V. All rights reserved.

1. Introduction

Zinc oxide (ZnO), which has a wide bandgap (3.4 eV) II–VI compound semiconductor, has a stable wurtzite structure with lattice spacing $a = 0.325$ nm and $c = 0.521$ nm. It has attracted many researchers for its unique properties and versatile applications in transparent electronics, ultraviolet (UV) light emitters, and piezoelectric devices [1,2]. ZnO has optical and electrical properties similar to GaN. Furthermore, it is relatively cheap, non-toxic, and resistant to radiation damage. An assortment of ZnO nanostructures, such as nanowires, nanotubes, nanorings, and nano-tetrapods have been successfully grown via a variety of methods including chemical vapor deposition, thermal evaporation, and molecular beam epitaxy (MBE) [3–5]. Among these methods, the thermal evaporation technique is the common method used to synthesize ZnO nanostructures at low cost and easy technology.

One-dimensional (1-D) semiconductor nanowires and nanorods have also attracted great attention because of their potential applications in both nanoscale electronic and optoelectronic devices [6,7]. In comparison to the bulk or thin film photodetectors, 1-D photodetectors should be able to provide a large response due to their larger aspect ratio of length to diameter and high surface to volume ratio. Kind et al. prepared ZnO nanowires by a vapor phase transport mechanism and then dispersed these ZnO nanowires directly onto the prefabricated gold electrodes [8]. Kang et al. found that the conductivity of these ZnO nanowires was very sensitive to UV light [9].

Photodetectors operating in the UV region are important devices that can be used in many commercial and military applications, such as ozone layer monitoring, flame detection and missile warning systems [9–11]. ZnO Schottky diodes and metal–semiconductor–metal (MSM) photodiodes detection in the UV region have also been realized [12]. Because many metals with high work function are not stable at high temperatures, there is a need to use a stable Schottky contact of wide bandgap. Palladium (Pd) has this ability and also it is a good conductor with superior thermal and chemical stabilities [13,14].

ZnO was mainly used in the past as transparent conductive electrodes and protective coatings. This has encouraged researchers to study the electrical properties of ZnO. Studying the optical properties, specifically photoelectric responses emerged much later; and there is much interest in fabricating ZnO nanostructures devices recently. Different methods have been employed to enhance photoconductivity in undoped ZnO films [15,16].

In this work, we have successfully fabricated Schottky photodetectors with high quality of undoped ZnO nanorods, which produced at low cost and simpler route through employing vapor–solid (VS) mechanism without catalyst at 850 °C. The details of the growth of the ZnO nanowires and the UV detector fabrication procedures are discussed below. The optical and electrical properties of the fabricated photodetectors are also elucidated below.

* Corresponding author. Fax: +60 4 6579150.
E-mail address: hind_alshaikh@yahoo.com (H.I. Abdulgafour).

0169-4332/$ – see front matter © 2011 Elsevier B.V. All rights reserved.
doi:10.1016/j.apsusc.2011.08.093

Author's personal copy

2. Experimental procedures

2.1. Synthesis of ZnO nanostructures

The synthesis process was carried out in a tube furnace (Thermolyne type F21100) with an inner diameter of 25 mm. N-type Silicon (Si) wafers with (1 0 0) orientation was used as a substrate. The wafers were single side polished. Prior to the synthesis process, the substrate was cleaned with acetone and isopropyl alcohol (IPA) in an ultrasonic bath, followed by rinsing with distilled water; and then the wafers were dried by nitrogen gas flow. The source material is pure metallic zinc fine powder (99.99%); the powder was placed in an alumina boat and the polished side of the Si wafer was facing to the powder. The furnace was initially heated up to 420 °C before inserting the boat and the wafers. Then the temperature was increased to 850 °C under the flow of highly pure argon and wet oxygen gases at a constant flow rate, 350 sccm.

2.2. ZnO nanostructures characterization

The surface morphology and structure of the ZnO nanostructures were examined by field emission scanning electron microscopy (FE-SEM). High-resolution X-ray diffractometer (HR-XRD) was used for phase identifications. The PL spectra of the ZnO nanostructures were measured using He–Cd laser with an excitation wavelength of 325 nm at room temperature. Keithley electrometer (Model 6517A) was used to record the *I–V* characteristics. All the experiments in this work were carried out under atmospheric pressure and at room temperature.

2.3. UV photodetectors fabrication and characterization

To fabricate UV photodetectors, Pd Schottky contact was deposited onto the sample surface of ZnO nanorods as shown in Fig. 1. A 160 nm thick Pd contact was subsequently deposited onto the ZnO nanorods by using A500 Edwards RF magnetron sputtering unit with the power of 150 W to serve as electrode metal contacts. The fingers of the Pd contact electrodes were 0.23 mm wide, 4 mm long with 0.4 mm spacing, and it consists of four fingers at each electrode to record the *I–V* relationships at different bias voltages from 5 V to −5 V. The tested fixture was placed with wires connected from the probes to Keithley device to measure the current–voltage (*I–V*) characteristics of the sample.

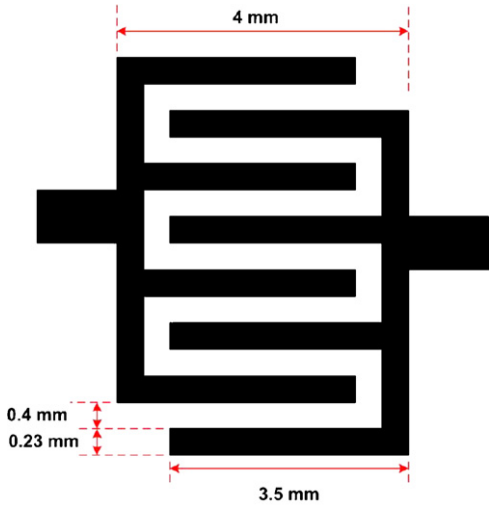

Fig. 1. Schematic diagram of the metal Pd Schottky contacts for ZnO MSM Photodetector.

3. Results and discussion

3.1. Structural characteristics

Fig. 2(a and b) shows the SEM images of the prepared ZnO nanorods structures grown under a constant flow rate, 350 sccm Ar/O_2 and at 850 °C. ZnO nanorods with high-density and good-quality were grown on Si substrate without a catalyst. Under these growth conditions, Fig. 2(b) indicates that the average length and diameter of these ZnO nanowires were around 2 μm, and 50–70 nm, respectively.

The produced samples were tested by HR-XRD to examine the crystal structure. Fig. 3 shows XRD pattern of the as-grown ZnO nanorods prepared by thermal evaporation technique at 850 °C. The ZnO nanorods are polycrystalline with a hexagonal close packed crystal structure. After oxidizing Zn in wet oxygen for 1 h, the diffraction patterns of zinc disappeared, and this revealed that the metallic zinc was completely transformed into ZnO.

Several peaks appeared at 2θ from 30° to 60° in the XRD pattern of the ZnO nanostructures, and they correspond to (1 0 0), (0 0 2), (1 0 1), (1 0 2) and (1 1 0) phases, respectively. The diffraction peaks can be indexed to the hexagonal structure of the ZnO according to JCPDS Card No. 01-089-7102. The lattice parameters are calculated to be $a = 0.3251$ nm and $c = 0.5210$ nm indicating that the products are pure ZnO. The strongest peak (0 0 2) at $2\theta = 34.37°$ with full-width half-maximum (FWHM) of 0.19° showed an excellent quality of the ZnO nanorods that the preferred growth orientation of nanorods is along the *c*-axis. Furthermore, the strong intensity and narrow width of the ZnO diffraction peaks also indicate that the resulting products had good crystallinity.

3.2. Optical properties

Fig. 4 depicts the PL spectrum of the ZnO nanorods at room temperature. It exhibits a strong peak at approximately 380 nm with a long tail in the long wavelength region. The strong PL

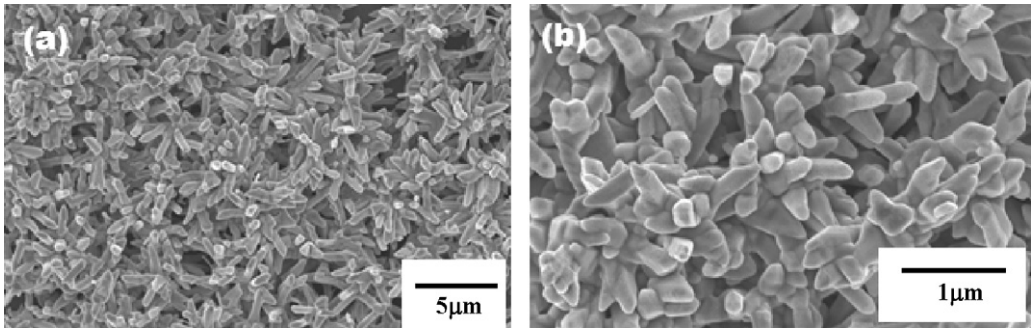

Fig. 2. Low and high SEM images of ZnO nanorods grown on a Si substrate at 850 °C.

Author's personal copy

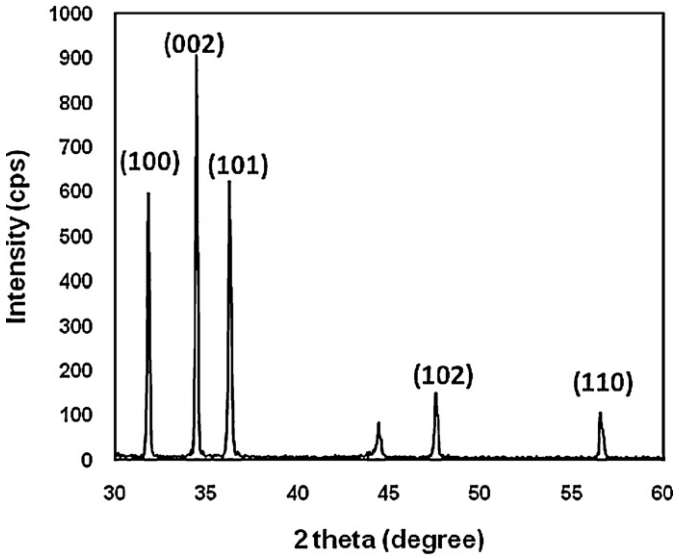

Fig. 3. The XRD pattern of the prepared ZnO nanorods at 850 °C grown temperature.

peak is attributed to the recombination of free excitons through exciton–exciton collision. UV emission is also called the near-band-edge (NBE) emission, due to the recombination of free excitons through an excitonexciton collision process. It has been suggested that deep level emissions are associated with the singly ionized oxygen vacancy in ZnO and results from the recombination of a photo-generated hole with the singly ionized charge state of this defect [17]. It was also found that full-width-half-maximum (FWHM) of the excitonic related PL peak is 17 nm.

In this study, the bandgap energy of ZnO nanostructures is focused at the UV near the band edge area. The estimated bandgap energy 3.225 (eV) from the PL peak of free exciton recombination 380 nm and using the equation, $E = hc/\lambda$ is false. The accurate relationship for emitted photon corresponding to free excitonic transition is $E_{photon} = hc/\lambda = Eg–Eix$, where Eix = 60 meV is the exciton energy formation in ZnO. Furthermore, it was found that the intensity ratio between the excitonic band and the green band emission was extremely large (140 times). In the other world, the intensity of the near band edge luminescence is around three orders

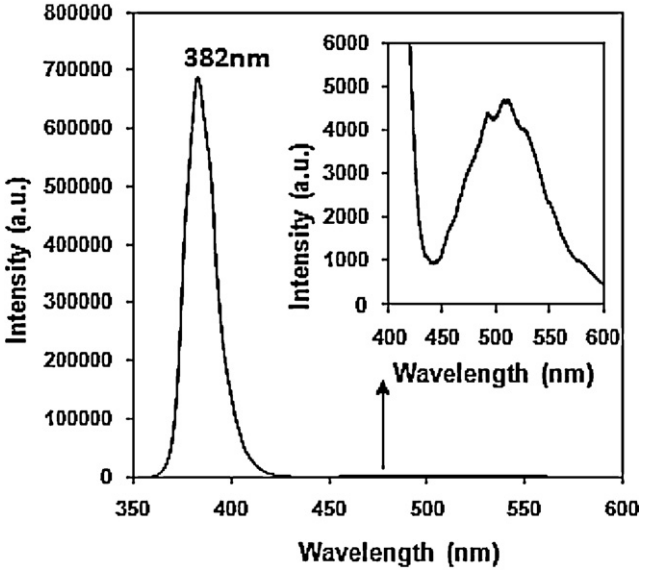

Fig. 4. PL spectrum and of ZnO nanorods grown at 850 °C.

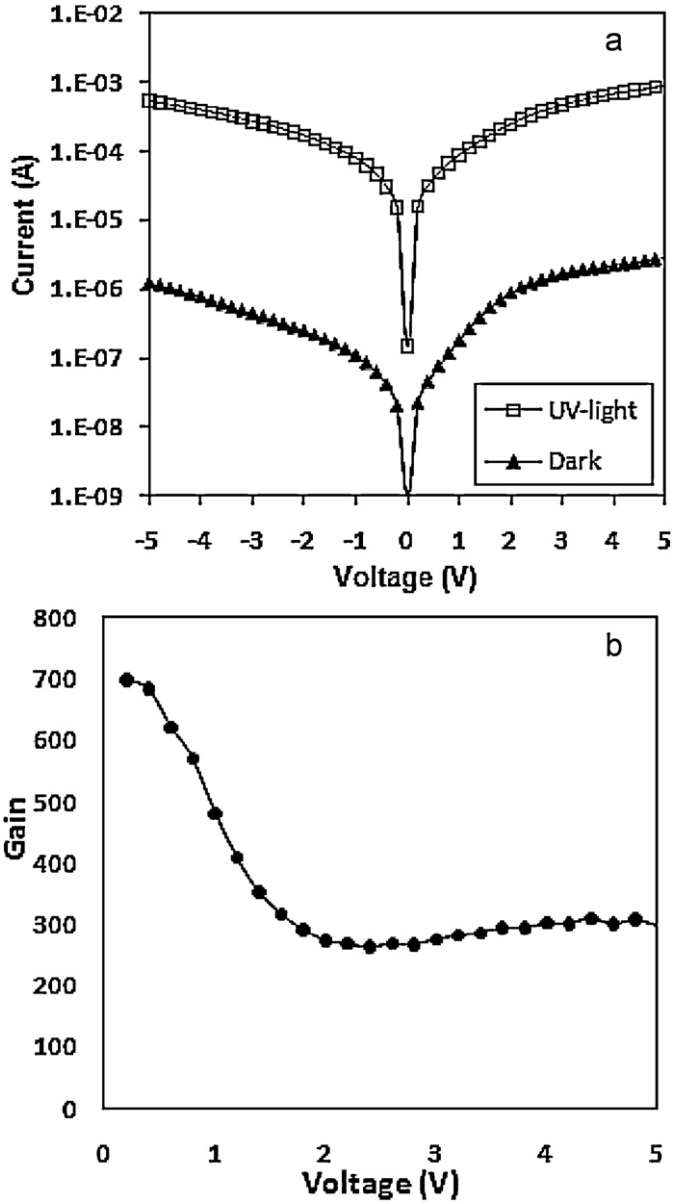

Fig. 5. (a) *I–V* current–voltage characteristics and (b) the gain, for undoped ZnO nanorods photodetector under UV and dark environment.

of magnitude higher as compared to the visible emission of the nanorods. From the literature, many researchers reported that the visible emission is a combination of red (~1.8 eV), yellow (~2.2 eV), and green (~2.5 eV) PL bands. Usually, the visible emission from ZnO is attributed to different defects such as oxygen vacancies (V_O), zinc vacancies (V_{Zn}) or a complex defect involving interstitial zinc (Zn_i) and interstitial oxygen (O_i) [18]. The extremely low intensity of the visible emission as compared to the near band edge emission in nanorods is an indication of low defect concentration. All these results indicate a good crystal quality of our ZnO nanostructures.

3.3. (*I–V*) characteristics

ZnO nanorods have been fabricated by vapor–solid (VS) mechanism without catalyst. Fig. 5 shows current–voltage (*I–V*) characteristics of the fabricated ZnO MSM UV photodiode, which comprised back-to-back Schottky diode from −5 V to 5 V with Pd electrodes, were measured in the dark, and under UV illumination. During the photocurrent measurements, the wavelength of

Author's personal copy

the excitation light was 365 nm and the incident optical power was 4 W. Under 5 V applied bias, it was found after annealing the sample at 400 °C for 5 min under flow of N_2 that the dark and UV current were 2.8×10^{-6} A, and 8.6×10^{-4} A, respectively. Furthermore, we calculated the photocurrent to dark current contrast ratio of our device with Pd electrode, the value of the UV light was found to be 307 times and about two orders of magnitude larger than the dark current. From the *I–V* measurements, it can be seen that the photocurrent increases with increase in the applied bias voltage. Previously, it has been reported that resistivity of the undoped ZnO nanowires was very large (>1 MΩ) [19]. In our undoped ZnO nanorods photodetector, we found that the load resistance under dark condition, and UV illumination is about 80.4 kΩ, and 23.5 kΩ, respectively, referring to the maximum allowed bias current. This load resistance is less than the one obtained by other authors [20]. The ability of the device to absorb the UV light was much higher than in the dark which implies that the UV light can be detected efficiently through these devices.

The Schottky barrier height can be derived from the *I–V* curves. The ϕ_B and n were determined by using thermionic emission equation [21]:

$$I = I_o \left[\exp\left\{\frac{qV}{nKT}\right\} - 1\right] \quad (1)$$

$$I_o = A^* A T^2 \exp\left\{-\frac{q\phi_B}{kT}\right\} \quad (2)$$

where I_o is the saturation current density based on thermionic emission theory, n is ideality factor, k is Boltzmann's constant, T is the absolute temperature, A^* is the effective Richardson coefficient, q is the absolute charge of electron and ϕ_B is the barrier height. In the calculation, the theoretical value of the effective Richardson coefficient of ZnO is $A^* = 32$ A/cm^2 K^2 [22], and thus A^* can be calculated as shown in the following equation:

$$A^* = \frac{4\pi m^* q k^2}{h^3} \quad (3)$$

where h is Planck's constant and $m^* \approx 0.27\, m_o$ is the effective electron mass of ZnO [23], n is the ideality factor. The Schottky contact area is 1.5×10^{-4} cm^2. The values of $n = 2.1$, and 1.5 for dark, and UV illumination, respectively were obtained from curve fitting. Using Eq. (2) and the theoretical value of A^*, under dark condition and UV illumination, the barrier height ϕ_B is estimated to be about 0.8 eV and 0.73 eV, respectively.

It was observed that the barrier height decreases from 0.8 eV to 0.73 eV with the incident UV light, accompanied by a significant improvement of the ideality factor n which decreases from 2.1 to 1.5, respectively. At the reverse bias of −1 V, the leakage current is 7.8×10^{-5} A and 1.08×10^{-7} A under UV illumination and dark, respectively. It was observed that the leakage current increases with the UV photocurrent. These observations suggest that the device exhibits a large photoconductive gain. The photoconductive gain is one of the most important physical parameters which determine the photocarrier collection efficiency. Previously, Carrano et al. has demonstrated that defects can cause photoconductive gain [23]. The large photoconductive gain seems to indicate the existence of a certain amount of defects in the ZnO nanorods [13].

The primary conduction mechanism in Schottky diodes, in general, is due to the flow of the majority charge carriers over the barrier by a thermionic process. The electrical characterization of a Schottky diode necessitates the determination of the barrier height and the ideality factor. For an ideal diode, the diode quality factor (n) should be nearly equal to unity [24].

Fig. 6 shows the spectral response of the photocurrent measurement on the MSM ZnO photodetector. Spectral responsivity measurements were also performed using a 2 mW xenon arc lamp as a light source and a monochromator. The light wavelength is 300 nm at 5 V applied bias. It was found that the maximum responsivity of the fabricated Pd/Zn MSM photodiode is 0.106 A/W. The quantum efficiency of our photodiode can be calculated by measuring the spectral response via:

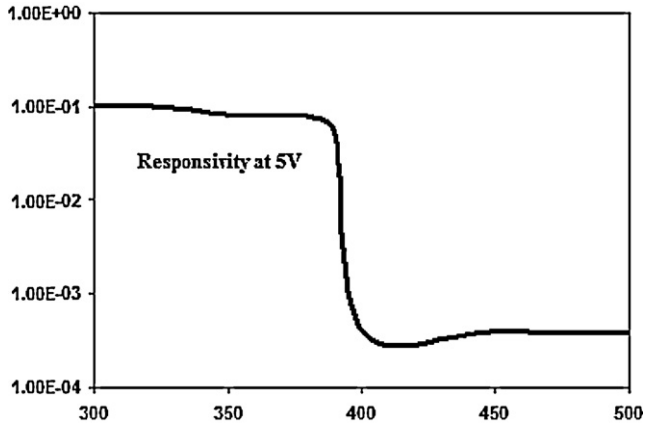

Fig. 6. Responsivity spectrum of the undoped ZnO nanorods photoconductor at room temperature under 5 V applied bias.

$$R = \eta \times \frac{q\lambda}{hc} \quad (4)$$

where η is the quantum efficiency, R is the measured responsivity, q is the electron charge, λ is the incident light wavelength, h is Planck constant, and c is the speed of light [25]. From Eq. (4), the quantum efficiency of our ZnO nanorods photodiodes is obtained which is around 43.8% at 300 nm. The cut-off occurred at 390 nm (see Fig. 6). The responsivity drops 2 orders of magnitude from 390 to 400 nm or by factor of 125 (I_{390}/I_{400}). The gradual cut-off at wavelength of 380 nm agrees with the nanoroads of ZnO band gap energy of 3.225 eV as shown in PL spectrum Fig. 4. This corresponds to the long wavelength cutoff of the device which is primarily determined by the absorption edge of ZnO [26]. We believe that the sensitivity of the derived ZnO nanorods in the UV region is good enough to be used in UV photodetector applications.

It is known that photoconduction of ZnO nanowire is governed by desorption and adsorption of oxygen. In the dark, oxygen molecules on the surface of the nanowires carry negative charges by capturing free electrons from the n-type ZnO. Thereby, it creates a depletion layer with low conductivity near the surface. UV light absorption generates electron–hole pairs [27]. The photogenerated holes oxidize the adsorbed negatively charged oxygen ions on the surface while the remaining electrons in the conduction band increase the conductivity. Thus, it is possible to achieve very rapid change in conductivity that was caused by photogenerated hole–electron pairs and their annihilation.

Fig. 7 shows the transient response of the device to UV light illumination at a bias of 1 V, 3 V, and 5 V. The device was allowed to stabilize and exposed to UV(365) nm illumination for duration of about 20 s within which the photocurrent was saturated. Rise time is defined as the time required to reach 90% from 10% of the maximum response value; while the fall time is the time needed to reach 10% from 90% of the maximum response. From Fig. 7, the rise time of the photoconductive device was obtained under different bias voltage 1 V, 3 V, and 5 V of about 2.8 s, 1.5 s, and 0.24 s, and the fall time was obtained to be 10.2 s, 8.2 s, and 3.6 s, respectively. One can also see from Fig. 7 that the intensity of the UV illumination increases with the increase of bias voltages.

The good response times are mainly attributed to the lack of in the presence of the deep levels from defects in the ZnO nanostructures. The fast response in an MSM detector is usually related

Author's personal copy

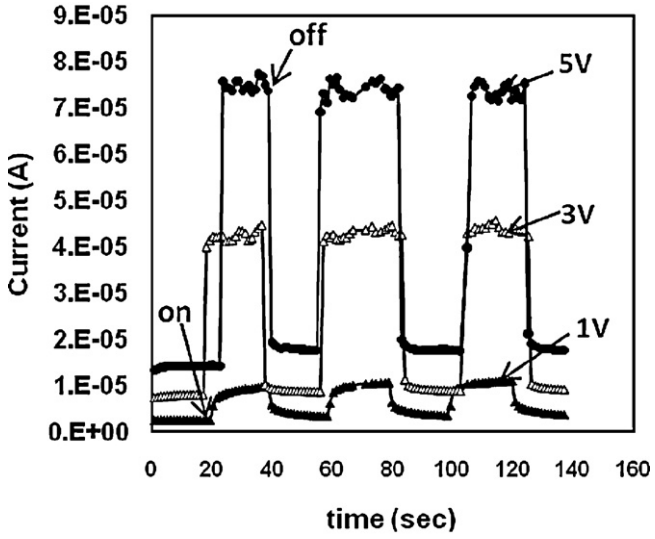

Fig. 7. Transient response of the photoconductor device to UV illumination. Under different bias voltages.

to the transit time of the photo-generated carriers; while the slow response in a ZnO MSM detector is usually attributed to the oxygen adsorption at the surface and grain boundaries [26,28].

4. Conclusion

In summary, we have reported the optical and photoelectric properties of undoped ZnO nanorods. The high crystal quality of ZnO nanorods was observed through the narrowest XRD (0 0 2) peak and the appearance of free exciton photoluminescence peak at room temperature. The static and transient photoresponses of the devices have been reported. The highest static response is about 0.106 A/W at 5 V bias for 365 nm light illumination. In a slow process at different bias voltages 1 V, 3 V, and 5 V, the rise time of Pd/ZnO is 2.8 s, 1.5 s, and 0.24 s, and the fall time was obtained to be 10.2 s, 8.2 s, and 3.6 respectively. The good response times are mainly attributed to the reduction of the deep levels of the defects in the ZnO nanostructures.

Acknowledgement

Financial support from the USM-RU-PRGS Postgraduate Research Grant under Universiti Sains Malaysia is gratefully acknowledged.

References

[1] W. Lee, M.C. Jeong, J.M. Myoung, Acta Mater. 52 (2004) 3949.
[2] A. Mang, K. Reimann, S.T. Ru¨benacke., Solid State Commun. 94 (1995) 251.
[3] T.M. Barnes, J. Leaf, S. Hand, C. Fry, C.A. Wolden, J. Appl. Phys. 96 (2004) 7036.
[4] H.I. Abdulgafour, Z. Hassan, N.H. Al-Hardan, F.K. Yam, Physica B 405 (2010) 4216.
[5] A. Setiawan, Z. Vashaei, M.W. Cho, T. Yao, H. Kato, M. Sano, K. Miyamoto, I. Yonenaga, H.J. Ko, J. Appl. Phys. 96 (2004) 3763.
[6] S. Liang, H. Sheng, Y. Liu, Z. Huo, Y. Lu, H. Shen, J. Cryst. Growth 225 (2001) 110.
[7] T.K. Lin, S.J. Chang, Y.K. Su, B.R. Huang, M. Fujita, Y. Horikoshi, J. Cryst. Growth 281 (2005) 513.
[8] H. Kind, H. Yang, B. Messer, M. Law, P. Yang, Adv. Mater. 14 (2002) 158.
[9] M. Kang, J.S. Lee, S.K. Sim, H. Kim, B. Min, K. Cho, G.T. Kim, M.Y. Sung, S. Kim, H.S. Han, Jpn. J. Appl. Phys. 43 (2004) 6868.
[10] E. Monroy, F. Calle, E. Munoz, F. Omnes, B. Beaumont, P. Gibart, J. Electron. Mater. 28 (1999) 240.
[11] S.J. Chang, T.K. Ko, Y.K. Su, Y.Z. Chiou, C.S. Chang, S.C. Shei, J.K. Sheu, W.C. Lai, Y.C. Lin, W.S. Chen, C.F. Shen, IEEE Sens. 6 (2006) 06–411.
[12] K. Sakurai, D. Iwata, S. Fujita, J. Appl. Phys. 38 (1999) 2606.
[13] F.D. Auret, S.A. Goodman, M. Hayes, M.J. Legodi, H.A. van Laarhoven, D.C. Look, Appl. Phys. Lett. 79 (2001) 3074.
[14] K.J. Duxstad, E.E. Haller, K.M. Yu, J. Appl. Phys. 81 (1997) 1.
[15] M. Liu, H.K. Kim, Appl. Phys. Lett. 84 (2004) 173.
[16] B.J. Jin, S.H. Bae, S.Y. Lee, B.J. Im, Mater. Sci. Eng. B 71 (2000) 301.
[17] S.C. Lyu, Y. Zhang, H. Ruh, H.J. Lee, H.W. Shim, E.K. Suh, C.J. Lee, Chem. Phys. Lett. 363 (2002) 134.
[18] C.C. Kim, J.H. Je, D.W. Kim, H.K. Baik, S.M. Lee, P. Ruterana, Mater. Sci. Eng. B 82 (2001) 105.
[19] C.L. Hsu, Y.R. Lin, S.J. Chang, T.S. Lin, S.Y. Tsai, I.C. Chen, Chem. Phys. Lett. 411 (2005) 221.
[20] Y.R. Lin, Y.K. Tseng, S.S. Yang, S.T. Wu, C.L. Hsu, S.J. Chang, Cryst. Growth Des. 5 (2005) 579.
[21] E.H. Rhoderick, R.H. William, Metal–Semiconductor Contacts, second ed., Oxford University Press, New York, 1998.
[22] R.E. Hummel, Electronic Properties of Materials, Springer, Berlin, 1992, p. 373.
[23] J.C. Carrano, P.A. Grudowski, C.J. Eiting, R.D. Dupuis, J.C. Campbell, Appl. Phys. Lett. 70 (1997) 1992.
[24] S.J. Young, L.W. Ji, R.W. Chuang, S.J. Chang, X.L. Du, Semicond. Sci. Technol. 21 (2006) 1507.
[25] L.J. Mandalapu, F. Xiu, Z. Yang, J. Liu, Mater. Res. Soc. Symp. Proc. 891 (2006).
[26] Y. Takahashi, M. Kanamori, A. Kondoh, H. Minoura, Y. Ohya, Jpn. J. Appl. Phys. 33 (1994) 6611.
[27] Q.H. Li, T. Gao, Y.G. Wang, T.H. Wang, Appl. Phys. Lett. 86 (2005) 123117.
[28] D.H. Zhang, J. Phys. D 28 (1995) 1273.